



## **PSEUDO-DYNAMIC TEST OF A FULL-SCALE CFT/BRB FRAME: PART 1- PERFORMANCE BASED SPECIMEN DESIGN**

**Keh-Chyuan TSAI<sup>1</sup>, Yuan-Tao WENG<sup>2</sup>, Sheng-Lin LIN<sup>3</sup>, and Subhash GOEL<sup>4</sup>**

### **SUMMARY**

This is the first of a three-part paper describing a full-scale 3-story 3-bay CFT buckling restrained braced frame (CFT/BRB) specimen that was constructed and tested in the structural laboratory of National Center for Research on Earthquake Engineering (NCREE) in Taiwan using pseudo dynamic test (PDT) procedures and internet testing techniques in October of 2003. The frame was tested using the pseudo-dynamic test procedures applying input ground motions from the 1999 Chi-Chi and 1989 Loma Prieta earthquakes, scaled to represent 50%, 10%, and 2% in 50 years seismic hazard levels. This paper describes the displacement-based seismic design procedures adopted in the design of the structural members. A target story drift limit of 0.025 radian for the 2% in 50 years hazard level governs the design strength of the frame. Nonlinear analyses illustrate that the response of individual BRB member can be satisfactorily simulated by using truss elements implemented in two different general purpose nonlinear response analysis programs PISA3D and OpenSees. Pre-test nonlinear dynamic analyses suggest that the peak story drift is likely to reach 0.025 radian after applying the 2/50 design earthquake on the frame specimen. CFT columns hinging at the base are expected, but should not fail as the rotational demand is moderate. Analytical floor displacement and story shear time history response predictions were web-cast during the PDTs. Tests confirmed that the PISA3D and OpenSees analyses predicted the experimental peak shears extremely well. Experimental peak lateral floor displacements well agree with the prescribed target design responses for both the 10/50 and 2/50 two events. Tests also confirmed that experimental peak inter-story drifts of 0.019 and 0.023 radians well agree with the target design limits of 0.02 and 0.025 radians prescribed for the 10/50 and 2/50 events, respectively.

### **INTRODUCTION**

Through international collaboration between researchers in Taiwan and the United States, a full-scale 3-story 3-bay RC column and steel beam RCS composite moment frame has been tested in October of 2002 in the structural laboratory of National Center for Research on Earthquake Engineering (NCREE) in

---

<sup>1</sup> Director, National Center for Research on Earthquake Engineering, Taipei, Taiwan, Email: kctsai@ncree.gov.tw

<sup>2</sup> Post-Doctoral Researcher, National Center for Research on Earthquake Engineering, Taipei, Taiwan

<sup>3</sup> Graduate Student, National Taiwan University, Taipei, Taiwan

<sup>4</sup> Professor, University of Michigan, Ann Arbor, MI, USA

Taiwan in October 2002 [1]. In the year 2003, a full-scale 3-story 3-bay CFT column with the buckling restrained composite frame (CFT/BRBF) specimen has been constructed and tested in October in a similar manner. The 3-story prototype structure is designed for a highly seismic location either in Taiwan or United States. The typical bay width of 7m and typical story height of 4m have been found common in Taiwan and US building configuration, it also corresponds well with the 1m spacing of the tie down holes on the strong floor and reaction wall of the lab. The total height of the frame, including the grade beam, is within the strong wall height 15m. The 2150mm wide concrete slab is adopted to develop the composite action of the beams. Measuring 12 meters tall and 21 meters long, the specimen is among the largest frame tests of its type ever conducted. The frame will be tested using the pseudo-dynamic test procedures applying input ground motions from the 1999 Chi-Chi and 1989 Loma Prieta earthquakes, scaled to represent 50%, 10%, and 2% in 50 years seismic hazard levels. Following the pseudo-dynamic tests, if no brace is fractured, quasi-static loads will be applied to cyclically push the frame to large inter-story drifts up to the failure of the braces, which will provide valuable data to validate possible failure mechanism and analytical models for large deformation response. Being the largest and most realistic composite CFT/BRB frame ever tested in a laboratory, the test provides a unique data set to verify both computer simulation models and seismic performance of CFT/BRB frames. This experiment also provided great opportunities to explore international collaboration and data archiving envisioned for the Networked Earthquake Engineering Simulation (NEES) initiatives or the Internet-based Simulations for Earthquake Engineering (ISEE) [2] launched recently in USA and Taiwan, respectively. This paper focuses on the displacement-based seismic design procedures adopted in the design of CFT/BRB frame specimen. During the planning stage, extensive nonlinear dynamic analyses were also carried out in order to ensure the possible seismic demands would not exceed the force and displacement limits of the test facility. This paper describes the analytical models and evaluates the seismic performance observed from the simulation results. Inelastic static and dynamic time history analyses have been conducted using PISA3D[3] and OpenSees (Open System for Earthquake Engineering Simulation), developed at National Taiwan University and Pacific Earthquake Engineering Research Center (PEER), respectively.

## BASIC DESIGN INFORMATION OF CFT/BRB FRAME SPECIMEN

The large-scale, 3-story CFT/BRB frame shown in Fig. 1 is employed in this experimental research. The prototype three-story building consists of 6-bay by 4-bay in plane. The seismic force in the transverse direction is to be resisted by two CFT/BRB frames symmetrically positioned in the building as shown in Fig. 1. Prior to the frame test, a series of subassembly tests have been completed in the structural laboratory in NCEE and some recommendations have been concluded for the design of the connections. As shown in Fig. 1, the height of the CFT/BRB frame specimen measured from the top of the foundation is 12 m. Other design and analytical parameters include:

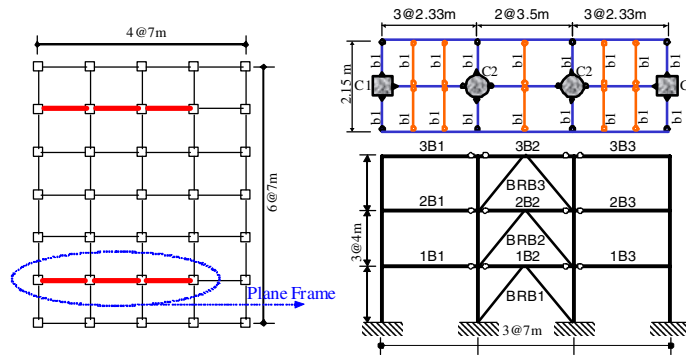


**Figure 1 Floor framing plan and elevation**

1. Loading

- (1) Dead Load: for the 1<sup>st</sup> and 2<sup>nd</sup> floor, it is 3.68 kN/m<sup>2</sup>; for the 3<sup>rd</sup> floor, it is 3.24 kN/m<sup>2</sup>  
 (2) Live Load: for all floors, it is 2.45 kN/m<sup>2</sup>

## 2. DESIGN CODES

- Taiwan seismic building code draft (2002, denoted as “Taiwan code 2002[4]”)
- All steel beams and CFT columns are designed by using AISC-LRFD[5]
- All P-M curves of the CFT columns for nonlinear frame response analysis are constructed using EC4 [6]

## 1. Design Load Combinations

- 1.2 DL + 0.5 LL + 1.0 EQ
- 0.9 DL + 1.0 EQ
- 1.2 DL + 1.6 LL

## 1. Story Seismic Mass: for the 1<sup>st</sup> and 2<sup>nd</sup> floors: 31.83 ton; 3<sup>rd</sup> floor: 25.03 ton (per CFT/BRB frame)

## 2. Materials

- Steel: All steel is A572 Gr.50,  $f_y=350$  MPa (50 ksi)
- Infill Concrete in CFT columns:  $f'_c=35$  MPa (5000 psi)

In the two identical prototype CFT/BRB frames, only the two exterior beam-to-column connections (Fig. 1) in each floor are moment connections, all other beam-to-column connections are assumed not to transfer any bending moment. The details of the moment connections are schematically given in Fig. 2 for the top through the first floor beams.

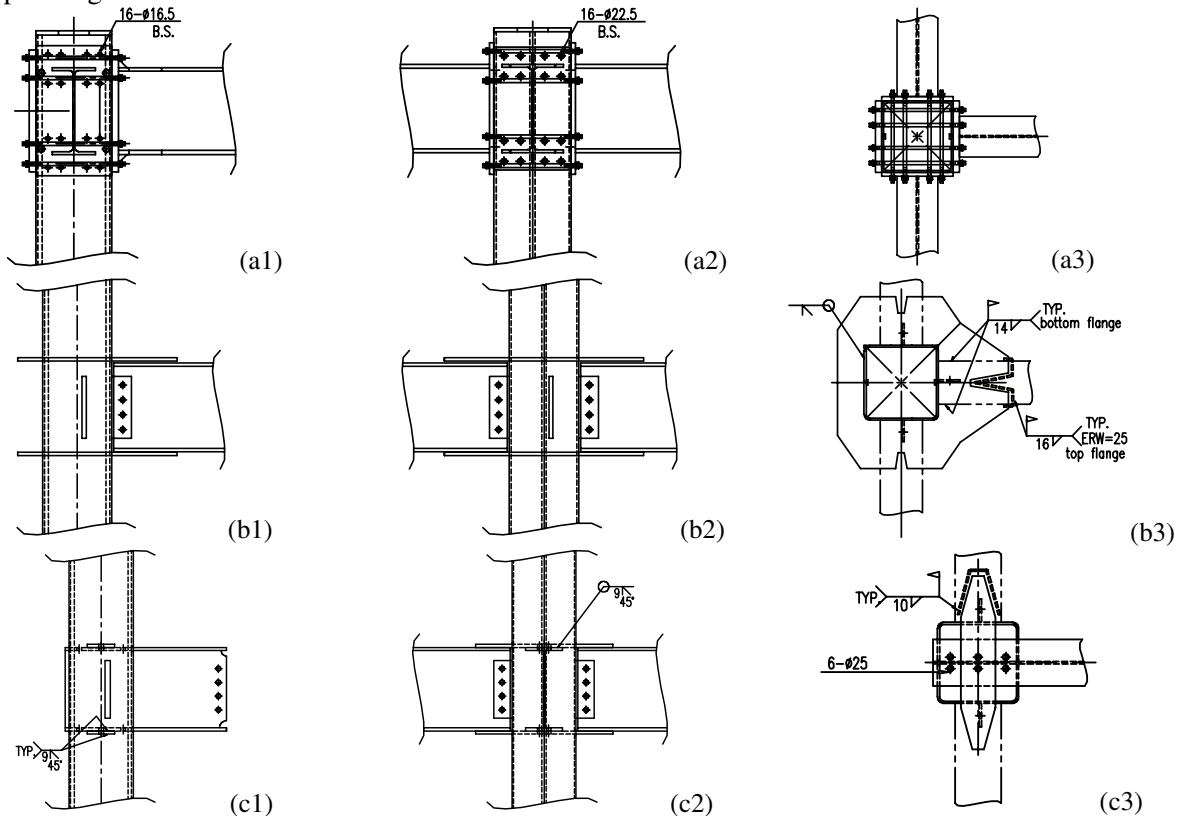


**Figure 2 Moment or pinned connections details (a, b, c for 3<sup>rd</sup>, 2<sup>nd</sup> and 1<sup>st</sup> floor, respectively)**

## DISPLACEMENT-BASED SEISMIC DESIGN PROCEDURE

This paper presents the results of applying the displacement-based seismic design (DSD) procedures (Loeding et al [7]; Medhekar and Kennedy [8]), to the design of the 3-story CFT/BRB frame specimen. The multi-mode design procedures adopted for this frame specimen were also studied and can be found in

the reference[8]. In this paper, it is assumed that the earthquake responses of the 3-story 3-bay CFT/BRB frame are essentially the first vibration mode. The DSD details follow:

## 1. Select acceptable (target) maximum story drift levels

### A. Design Earthquake Acceleration Response Spectra

Fig. 3a and Fig. 3b consider Taiwan seismic code draft updated in 2002. It stipulates, for a hard rock site, the  $S_a(T=1 \text{ sec})$  values for earthquake hazard of 10% chance of exceedance in 50 years (10/50 Design Earthquake, DE) and 2/50 (Maximum Considered Earthquake, MCE) earthquakes as 0.68g and 0.91g, respectively. These are the same as those used for the RCS frame tests in 2002. The 5% damped  $S_a$  values for TCU082EW records adopted in the RCS frame tests are also shown on Figs. 3a and 3b. The corresponding PGA values for the 10/50 and 2/50 levels of excitations are 0.46g and 0.62g, respectively, for the TCU082EW record. Similarly, for the LP89g04NS record, the corresponding PGA values for the 10/50 and 2/50 levels of excitations are 0.40g and 0.54g, respectively.

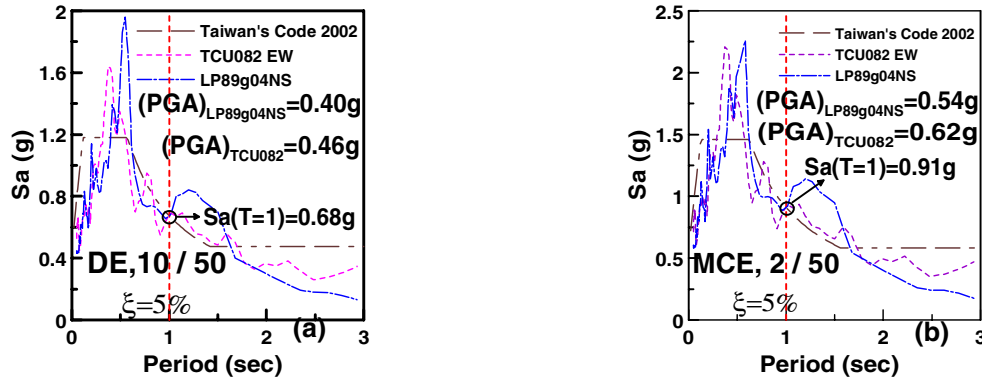


Figure 3 Design acceleration spectra (a)10/50 (b)2/50 hazard level

### B. Performance Criteria for the CFT/BRB Frame

Since no performance criteria, prescribed for the CFT/BRB frame system, can be found in the model seismic building design standards, the proposed performance criteria is chosen as indicated in Table 1 for the two hazard levels considered in this study. For the 10/50 and 2/50 events, the inter-story drift limits are set at 0.02 and 0.025 radians, respectively.

Table 1 Proposed building performance levels for the CFT/BRB frame specimen

	Building Performance
Life Safety (10/50-0.02 hazard/performance)	Many buckling restrained braces yield. Beam-to-column moment connection should not fail.
	Transient inter-story drift limit=0.02 radian Permanent inter-story drift limit=0.005 radian
Collapse Prevention (2/50-0.025 hazard/performance)	Extensive yielding of braces. Braces and its connections should not fail. Some beam-to-column moment connections may fail.
	Transient inter-story Drift limit=0.025 radian Permanent inter-story Drift limit=0.01 radian

## 2. Calculate the maximum displacement profile

It is assumed that structural first modal design displacement profile can be simplified as an inverted triangle. If a target drift level is selected in Step 1, then each story displacement can be decided. For example, under the 10/50 event, the story drift limit is 0.02 radian, thus the target roof displacement is

24cm; for the 2/50 event and the corresponding target drift angle of 0.025 radian, the target roof displacement is 30cm.

### 3. Calculate the system displacement

The system displacement is equal to the effective displacement and given by

$$\delta_{\text{eff}} = \sum_{i=1}^N m_i \delta_i^2 / \sum_{i=1}^N m_i \delta_i \quad (1)$$

where  $m_i$  is the story mass,  $\delta_i$  is the  $i^{\text{th}}$  target story displacement,  $N$  is the story number of the building, then  $\delta_{\text{eff}}$  is the effective displacement. This step essentially translates the actual MDOF structure to the substituted SDOF structure through displacements.

### 4. Estimate system ductility from the properties of buckling restrained braces

The relationship between brace deformation and inter-story drift angle is approximated as given by Eq. 2 and Fig. 4[9].

$$\varepsilon_{wp} = (\theta \cdot \sin 2\phi) / 2 \quad (2)$$

$$\frac{\varepsilon_c}{\varepsilon_{wp}} = \frac{1}{\frac{L_j A_c}{L_{wp} A_j} + \frac{L_t A_c}{L_{wp} A_t} + \alpha_c} = \gamma \quad (3)$$

where  $\theta$  is the story drift angle,  $\phi$  is the angle between the horizontal beam and the brace showed in Fig.4, and  $\varepsilon_c$  is the strain of the brace core segment,  $\alpha_c = L_c / L_{wp}$  ( $L_c$  and  $L_{wp}$  are defined in Fig. 5). When the braces yield,  $\varepsilon_c = \varepsilon_{cy} = f_{sy} / E_s$ , the  $i^{\text{th}}$  story drift  $\theta_{yi}$  corresponds to the brace yielding can be estimated as:

$$\theta_{yi} = 2 \cdot \varepsilon_{cy} / \gamma \cdot \sin 2\phi \quad (4)$$

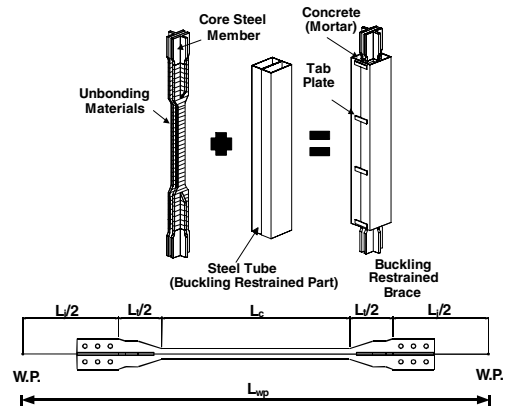
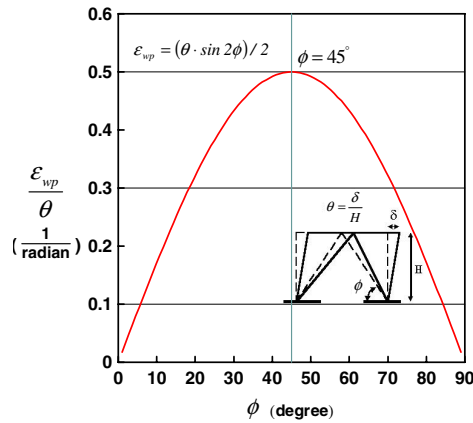


**Figure 4 brace strain versus story drift relationships Figure 5 Profiles of core steel in the BRB**

If  $\theta_{mi}$  is the target drift of the  $i^{\text{th}}$  story calculated from the target displacement profile, then the story ductility can be computed from:

$$\mu_i = \theta_{mi} / \theta_{yi} \quad (5)$$

After calculating all the story ductilities from Eq. 5, the average of all story ductilities can be taken as the system ductility. If the BRB is made from A572 Gr.50 steel, its minimum yield strain  $\varepsilon_{cy}$  is about 0.00172. Assume that the core length ratio  $\alpha_{ci}$  for braces at  $i^{\text{th}}$  floor is about 0.5, then the story ductility can be calculated by Eqs. 2 through 5, and the results show in Table 3a that the averaged system ductility

demands for the 10/50 and 2/50 events are 9.19 and 11.5, respectively. The actual material test results given in Table 2 can be used to refine the estimations of the ductility demand. Given the actual steel core strength and the length ratio  $\alpha_{ci}$  for braces at 1<sup>st</sup>, 2<sup>nd</sup> and 3<sup>rd</sup> floor as 0.60, 0.49 and 0.57, respectively, then the story ductility and the averaged system ductility demands (shown in Table 3b) for the 10/50 and 2/50 events are 7.28 and 9.10, respectively.

**Table 2 Material test results**

		Positions of Sampling		f <sub>y</sub> (MPa)	f <sub>u</sub> (MPa)
Steel (A572Gr.50)	3FL	Beam	Flange	372	468
			Web	426	493
		BRB3	core steel material	373	483
	2FL	Beam	Flange	414	503
			Web	482	538
		BRB2	core steel material	397	545
	1FL	Beam	Flange	370	486
			Web	354	485
		BRB1	core steel material	421	534
C1(Tube-400-9)		Steel		374, 488	488
		Concrete		f <sub>c</sub> '=35 MPa	
C2(Pipe-400-9)		Steel		543	584
		Concrete		f <sub>c</sub> '=35 MPa	

**Table 3 Computation of story ductility and system ductility**

(a) All steel material strength are nominal

Story	$\alpha_{ci}$	Story Ductility					
		10/50			2/50		
		$\theta_{yi}$	$\theta_{mi}$	$\mu_i$	$\theta_{yi}$	$\theta_{mi}$	$\mu_i$
		unit : 1/1000 rad			unit : 1/1000 rad		
3F	0.50	1.74	20	9.19	1.74	25	11.5
2F	0.50	1.74	20	9.19	1.74	25	11.5
1F	0.50	1.74	20	9.19	1.74	25	11.5
Average		1.74	20	9.19	1.74	25	11.5

(b) All steel material strength are based on tensile coupon test results

Story	$\alpha_{ci}$	Story Ductility					
		10/50			2/50		
		$\theta_{yi}$	$\theta_{mi}$	$\mu_i$	$\theta_{yi}$	$\theta_{mi}$	$\mu_i$
		unit : 1/1000 rad			unit : 1/1000 rad		
3F	0.57	2.42	20	6.61	2.42	25	8.27
2F	0.49	1.96	20	8.15	1.96	25	10.2
1F	0.60	2.26	20	7.08	2.26	25	8.85
Average		2.21	20	7.28	2.21	25	9.10

## 5. Compute the effective structural vibration period

Applying the  $R_y - \mu - T$  relationships suggested by Newmark and Hall[9]:

$$S_{d,in} = \frac{\mu}{R_y} \left( \frac{T}{2\pi} \right)^2 S_a = \frac{\mu}{R_y} S_d \quad (6)$$

Eq. 6 provides a convenient way to determine the deformation of the inelastic system from the elastic design spectrum, where  $S_{d,in}$  is the inelastic peak deformation of the SDOF system,  $S_a$  and  $S_d$  are the

elastic design spectral acceleration and displacement, respectively,  $R_y$  is the yield strength reduction factor. For the smoothened design response spectra given in Fig. 4 for a hard site, it is stipulated in the latest Taiwan seismic force design standards that:

$$R_y = \begin{cases} \mu & ; T \geq T_0 \\ \sqrt{2\mu-1} + (\mu - \sqrt{2\mu-1}) \times \frac{T-0.6T_0}{0.4T_0} & ; 0.6T_0 \leq T \leq T_0 \\ \sqrt{2\mu-1} & ; 0.2T_0^D \leq T \leq 0.6T_0 \\ \sqrt{2\mu-1} + (\sqrt{2\mu-1} - 1) \times \frac{T-0.2T_0}{0.2T_0} & ; T \leq 0.2T_0 \end{cases} \quad (7)$$

$$T_0^D = S_{D1}/S_{DS} \quad ; \quad T_0^M = S_{m1}/S_{MS} \quad (8)$$

where corner period is  $T_0 = T_0^D$  (for 10/50) or  $T_0^M$  (for 2/50). It should be noted that for the 10/50 event (Fig. 3a),  $S_{DS} = 1.18g$  and  $S_{D1} = 0.68g$ , while for the 2/50 event (Fig. 3b),  $S_{MS} = 1.46g$  and  $S_{m1} = 0.91g$ . Using Eqs. 6 through 8 and applying the system ductility demands 7.28 and 9.10, inelastic displacement response spectra  $S_{d,in}$  can be constructed as shown in Fig. 6 from the response spectra given in Figs. 3a and 3b for the two noted earthquake hazards. Applying the target displacement profile for the 10/50 event using Eq. 1, the effective displacement  $\delta_{eff}$  is 0.18 m. Similarly, for the 2/50 event, the effective displacement is 0.23 m. Intersecting the effective target displacements of 0.18 m and 0.23 m on the inelastic displacement response spectra shown in Fig. 6, the effective first vibration period  $(T_{eff})_1$  during the 10/50 and 2/50 events can be found as 1.42 and 1.32 second, respectively. Noted that for the 10/50 design hazard against a roof drift limit of 0.02 radian, the system appears to be less demanding in terms of strength and stiffness, thus have resulted in a lighter design, than that for the 2/50-0.025 hazard/performance criteria. This could help in explaining why the  $(T_{eff})_1$  values for two different designs, during the 10/50 and 2/50 events, are found as 1.42 and 1.32, second, respectively. In Fig. 6, the elastic displacement response spectra ( $\mu=1.0$ ) are also given.

## 6. Calculate the effective mass

The effective mass is calculated by Eqs. 9 and 10:

$$c_i = \delta_i / \delta_{eff} \quad (9)$$

$$m_{eff} = \sum_{i=1}^N m_i c_i \quad (10)$$

## 7. Calculate the effective stiffness $K_{eff}$ :

$$K_{eff} = 4\pi^2 m_{eff} / (T_{eff})_1^2 \quad (11)$$

## 8. Calculate the design base shear

The design yield base shear  $V_d$  is calculated from Eqs. 12 and 13:

$$V_b = K_{eff} \times \delta_{eff} \quad (12)$$

$$V_d = V_b / [1 + \alpha_h (\mu - 1)] \quad (13)$$

where  $\alpha_h$  is the bilinear stiffness ratio, generally  $\alpha_h$  can be taken as 0.1. The design base shears, 1575 and 2057 kN represent the stage of significant system yielding for the two events. It is evident that the 2/50-0.025 hazard/performance criteria govern the design. For the purposes of research, separate studies also investigated the seismic demands imposed on different frames designed for both the 10/50 and 2/50 hazard levels considering various design story force computation strategies[10].

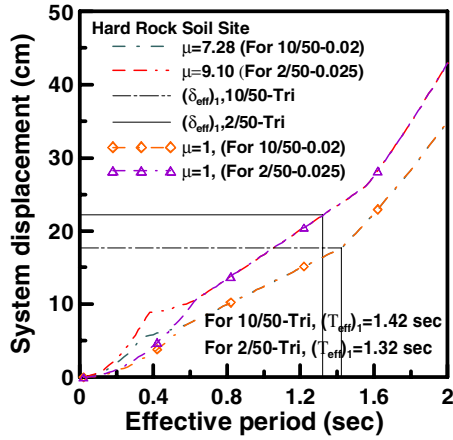


Fig.6 Inelastic Design Displacement Spectra

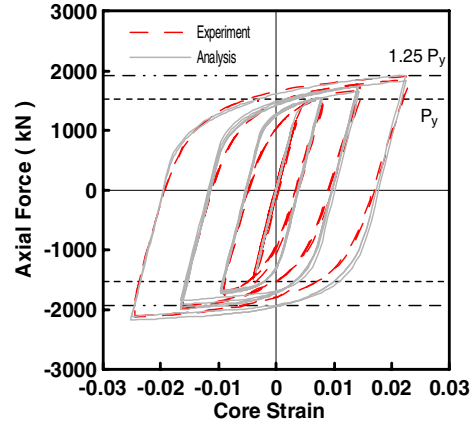


Fig.7 Force versus Core Strain Relationship of BRB using A572 Gr.50

## 9. Distribute the design base shear over the frame height

The design base shear is distributed over the frame height using Eq. 14 to get the lateral design story forces.

$$F_i = m_i \delta_i V_d / \sum_{i=1}^N m_i \delta_i \quad (14)$$

Since the system ductility affects design base shear as shown in Eq. 13, the triangular story force distributions are listed in Table 4 for four different designs considering the two hazard levels (10/50 and 2/50) and the two material strengths (nominal A572 GR50 versus the tensile coupon strengths). Frames 10/50-Tri and 2/50-Tri consider the brace nominal strength and triangular force distribution for the 10/50 and 2/50 events, respectively. Frames 10/50-TriMR and 2/50-TriMR denotes the designs using the actual material strength. The 28-day 5000 psi (35 MPa) concrete nominal compressive strength for CFT columns is considered in all the frame designs. The cylinder test results will be adopted in future analysis. However, the effects of its variations are believed less significant at this stage as most of the story shears should be resisted by steel BRBs. Table 4 also gives the four different frame fundamental periods results from the variation of the designed cross-sectional area along the length of the brace. Details will be further discussed below.

Table 4 Comparison of design lateral story forces and elastic period

Story	Lateral Story Force (kN)			
	Frame 10/50-Tri	Frame 10/50-TriMR	Frame 2/50-Tri	Frame 2/50-TriMR
3F	620.6	693.4	786.2	889.8
2F	526.2	587.9	666.5	754.3
1F	263.1	293.9	333.3	377.2
Sum	1409.9	1575.2	1786.0	2021.3
Elastic Period (sec)	0.70	0.72	0.68	0.70

## 10. Conduct structural analysis and design the members for the CFT/BRB frame

Assume 80% of the total horizontal shear at each story is resisted by two BRBs, therefore, the preliminary selection of the core cross sectional area  $A_c$  of BRBs can be determined from the following:



$$A_c = P_{brace} / F_y \quad (15)$$

Since the BRBs are the primary energy dissipation element under the two levels of earthquake, the connecting beams and the column members need to be designed considering the capacity design requirements. Fig. 7 gives typical force versus deformation responses with respect to the actual yield capacity ( $A_c \times F_{y,actual}$ ) for BRB specimens tested in National Taiwan University using A572 Gr.50 steel [11]. It is evident that under large cyclic increasing strains, the peak compressive force responses are slightly larger than tensile force responses. In addition, the strain hardening effects factor of Grade 50 steel is about 1.25 (for typical A36 steel, strain hardening factor can reach 1.5). Therefore, the maximum possible brace force can be estimate as follows:

$$P_{max} = \beta \times \Omega \times \Omega_h \times P_y \quad (16)$$

where  $P_y$  is the nominal tensile yield strength,  $\Omega$  accounts for possible material overstrength,  $\Omega_h$  represents the effects of strain hardening, and  $\beta$  (of about 1.1) considers the ratio between the peak compressive and tensile forces. Since the actual yield strength obtained from the tensile coupon tests will be employed to adjust the final BRB cross sectional area before fabrication, the material overstrength factor is eliminated in the capacity design of members or connections for the CFT/BRB frame specimen. The beams given in Table 5 satisfy the capacity design principle. It considers the horizontal brace force components as beam axial loads and the flexural demand resulted from a vertical unbalanced concentrated force of  $0.1\Omega_h P_y \sin \phi$  acting upward at the center of the beam span as depicted in the free body diagram

Fig. 8. The LRFD specifications apply:

$$P_u / (\phi_c P_n) \geq 0.2 : \quad P_u / (\phi_c P_n) + \frac{8}{9} M_u / \left[ \left( 1 - \frac{P}{P_e} \right) \phi_b M_n \right] \leq 1.0 \quad (17)$$

where  $P_n = F_{cr} A_g$ ,  $P_e = \frac{\pi^2 EI}{(kl)^2}$ ,  $\phi_c = 0.75$  (tension) or  $0.85$  (compression),  $\phi_b = 0.9$

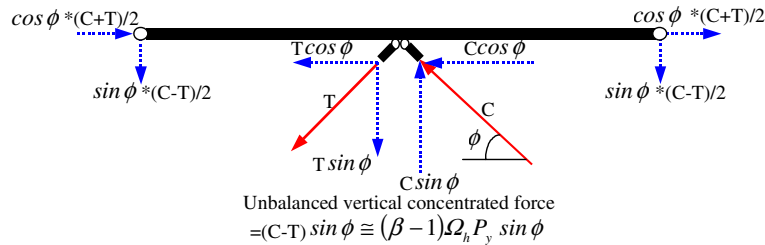


**Figure 8 Free Body Diagram of a Beam Supporting the**

Note that the bottom beam flange is not laterally braced except by transverse beams at the center point of span. Accordingly,  $P_n$  and  $M_n$  in Eq. 17 are conservatively computed (without considering the effects of the concrete slab) from an unbraced length of 3.5 m for the capacity design of left beam segment shown in Fig. 8. The selection of the two interior columns is concrete filled 400 mm diameter steel pipe with a wall thickness of 9 mm, while the two exterior CFT columns are 350 mm square 9 mm thick. The 28 days compressive strength of concrete is 5000 psi (35 MPa). The beams in the two end bays in each floor are chosen the same as the interior bay. In order to simplify the construction and the behavior of the specimen, only the exterior beam ends are moment connected to the exterior column. At all beam-to-column moment connecting joints, the strong column weak beam and strong panel zone weak beam criteria are satisfied. It meets the requirements of simultaneously applying a strain hardening factor of 1.1 and a factor of 1.25 to account for the concrete slab effects on the bare steel beam nominal flexural capacity. This demand is checked against the column or panel zone strength without adopting the strength reduction factor. An elastic model was then constructed using the SAP2000N[11] program to check the distributions of the story shear in the braces and columns. The elastic axial stiffness computation of the CFT columns follows the LRFD specifications. The effects of flexural stiffness of the CFT columns have been investigated by

considering the full composite or bare steel section. After very few iteration, it is found in the elastic model that the final selection of the braces and other member for Frame 2/50-TriMR shown in Table 5 satisfy all the requirement noted above. In particular, the BRBs in each story will reach yielding at the proximity of the design story shear. The total core cross sectional area for each individual brace is 15, 25 and 30 cm<sup>2</sup> for the 3<sup>rd</sup>, 2<sup>nd</sup> and 1<sup>st</sup> story, respectively. The fundamental vibration period of the four design results noted above ranges from 0.68 to 0.72 second. In addition, the effects of varying the flexural stiffness of the CFT columns from fully composite (using LRFD specification [5]) to the bare steel have been found insignificant, only change the fundamental vibration period from 0.68 to 0.71 second. Consequently, an averaged CFT flexural stiffness (resulting in a fundamental period of 0.70 second) has been adopted in all the analysis presented herein.

**Table 5 Comparison of member sizes of CFT/BRB frame specimen**

Frame Label		Core Cross Sectional Area of Braces (A572 GR50) unit : cm <sup>2</sup>					
		1FL (BRB1)		2FL (BRB2)		3FL (BRB3)	
2/50-Tri		34		27		15	
2/50-TriMR		30		25		15	
Dimension of Columns (A572 GR50) unit : mm				C1: Tube: 350×9, C2: Pipe: 400×9			
Dimension of Beams (A572 GR50) unit : mm							
3FL	3B1~3B3:H400×200×8×13		2FL	2B1~2B3:H450×200×9×14		1FL	1B1~1B3:H456×201×10×17

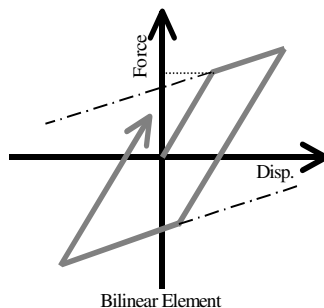
Three different types of moment connections, namely through beam, external diaphragm and bolted end plate types, varying from the first floor to the third floor are chosen and fabricated for the exterior beam-to-column connections (Fig. 2). Three types of BRBs, including the single-core, double-cored and the all-metal BRBs, have been installed in the three different floors. In particular, two single-cored unbonded braces (UBs), each consisting of a steel flat plate in the core, were denoted by Nippon Steel Company and have been installed in the second floor. Each UB end to gusset connection uses 8 splice plates and 16-24mm $\phi$  F10T bolts. The two BRBs installed in the third floor are double-cored constructed using cement mortar infilled in two rectangular tubes [13] while the BRBs in the first floor are also double-cored but fabricated with all-metal detachable features [11]. Each end of the double-cored BRB is connected to a gusset plate using 6- and 10-22mm $\phi$  F10T bolts at the third and first floor, respectively.

## ANALYTICAL MODELS

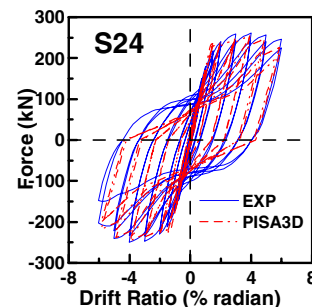
In this section, the structural member and properties are based on Frame 2/50-TriMR (Tables 2 and 5) using PISA3D and OpenSees.

### PISA3D model

All BRBs were modeled using the two-surface plastic (isotropic and kinematic) strain hardening truss element (Fig. 9). All the beam members were modeled using the bi-linear beam-column elements (Fig. 10). Consider the strength degrading behavior of the concrete, All the columns members were modeled using the three-parameter degrading beam-column elements[3]. It is evident that the hysteretic behavior of CFT column members simulated by PISA3D shown at Fig.11 is satisfactory and well agree with the experimental results obtained in the DSCFT column specimen S24 cyclic load test[14]. A leaning column is introduced in the frame model in order to simulate the 2<sup>nd</sup> order effects developed in the gravity columns.



**Fig. 10 Bilinear element model**



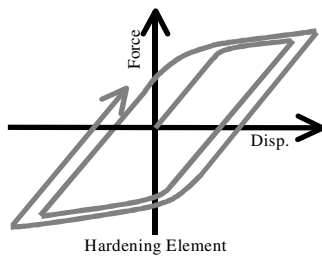


**Fig. 9 Two-surface plasticity hardening truss element OpenSees Model**

All the CFT columns and steel beams of the frame were modeled using the flexibility-based nonlinear beam-column element with discretized fiber section model as illustrated in Fig. 12. All BRBs were modeled using the truss element with bilinear isotropic strain hardening. A leaning column arrangement has also been adopted in OpenSees model.

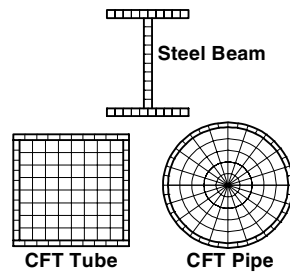


**Fig. 12 Fiber sections in OpenSees**

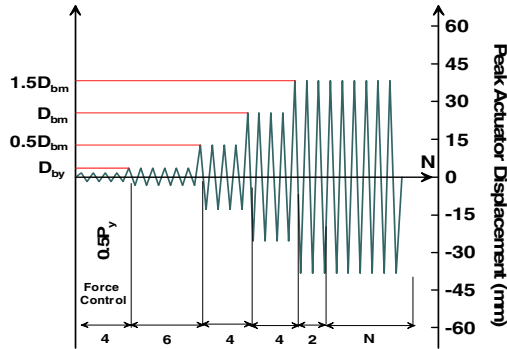


**Fig.13 Cyclic axial displacement history for two-surface plasticity brace element (core length=1700mm)**

**Fig. 11 Force-Disp. curves of CFT columns**

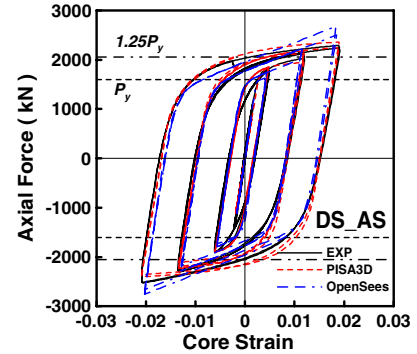


**Fig. 14 BRB element models**

### Element Responses

Cyclic analyses on basic elements are exercised to verify the differences of the elements adopted in PISA3D and OpenSees. Cyclic axial displacement history given in Fig. 13 was applied to two different truss elements in order to validate the analytical BRB models. It is evident that the hysteretic behavior of BRB member simulated either by PISA3D or OpenSees shown at Fig.14 is satisfactory and well agree with the experimental results obtained in a NTU test using A572 Gr.50 BRB [11]. Similarly, in order to compare the three-parameter degrading beam-column element implemented in the PISA3D program and the fiber CFT beam-column models in the OpenSees program, the results of simulating the strength degrading and hysteretic behaviors of the DSCFT column specimen S24 shown at Fig. 11. In addition, since most of the story shear is resisted by the braces, preliminary analyses have confirmed that the effects of the CFT column hysteretic behavior are rather insignificant.

## NONLINEAR ANALYSIS AND SEISMIC DEMAND EVALUATIONS

As noted above, two ground accelerations, TCU082EW and LP89g04NS shown in Fig. 15 were adopted in the RCS frame tests in 2002 [1]. In addition, similar to the earthquake intensities and sequence arranged for RCS frame tests, Fig. 16 shows the arrangement of the earthquake sequence adopted in studying the effects of four continuous earthquake events. These four events are 50/50 (using TCU), 10/50 (using LP), 2/50 (using TCU), another 10/50 (using LP). However, the experiment was forced to pause twice because of two unexpected accidents, one is that out of plane buckling of a gusset plate at the BRB-to-beam connection was detected at the 1<sup>st</sup> story, another is that cracks on the top of a RC foundation around the gusset plate at the BRB-to-column joint. Therefore, a total of six pseudo dynamic tests(PDT) were conducted. Fig. 17 presents the ground accelerations applied in the six PDTs. After the pseudo dynamic tests, all the BRBs were not damaged. Therefore, cyclic increasing story drifts (Fig. 18) were imposed until the failure of the BRBs. When the BRBs were failed either in fracturing of BRBs or

buckling in the gussets [15], the minimum CPD of BRBs is 167 while the maximum is about 212, close to the cumulative ductility capacity observed in the typical BRB component tests [11].

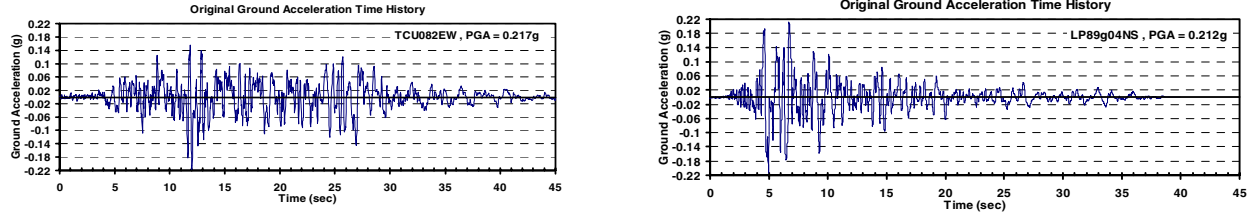


**Fig. 15 Original ground accelerations used in test (before scaling)**  
50/50 event → 10/50 event → 2/50 event → 10/50 event

TCU082 EW → LP89g04 NS → TCU082 EW → LP89g04 NS

**Fig. 16 Earthquake sequence applied in this study**

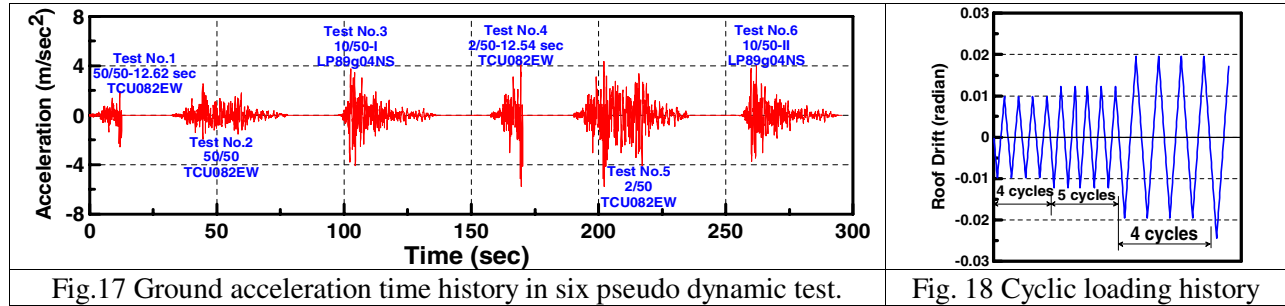


**Fig.17 Ground acceleration time history in six pseudo dynamic test.**

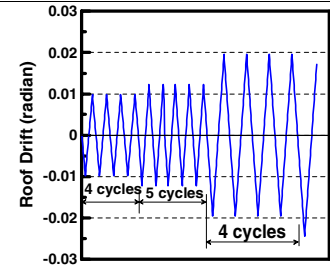


**Fig. 18 Cyclic loading history**

Fig. 19 and Fig.20 present the roof displacement time history and inter-story drift and story shear relation of 1<sup>st</sup> story of CFT/BRBF specimen imposed in the test No.5, the peak value of roof displacement is about 208mm and story drift at 1<sup>st</sup> story is 0.025radian approximately. It is evident that the hysteretic behavior of CFT/BRBF simulated either by PISA3D or OpenSees shown at Fig.19 and Fig.20 is satisfactory and agree with the experimental results. Fig. 21 shows the peak story shear distributions under the applications of 50/50, 10/50 and 2/50 three earthquake load effects. It is confirmed that the PISA3D and OpenSees analyses have predicted the experimental peak shears extremely well. Fig. 22 shows that except the roof floor, experimental peak lateral floor displacements well agree with the target design responses for both the 10/50 and 2/50 two events. Tests (Fig. 23) also confirmed that experimental peak inter-story drifts of 0.019 and 0.023 radians well agree with the target design limits 0.02 and 0.025 radians prescribed for the 10/50 and 2/50 events, respectively. The ratios between the cumulative inelastic axial deformation and the tensile yield displacement [17] can be defined as CPD. In this study, it is taken as the plastic deformations occurring in a brace summed over all cycles throughout the entire response history, in either tension or compression, divided by the tensile yield displacement of the BRB brace member. The results for each BRB are listed in Table 6. It analytical peak value reaches 68.8 after undergoing the four earthquake events, at one of the 3<sup>rd</sup> floor brace predicted by PISA3D. Table 7 presents the CPD value of the same brace reached 78.0 after undergoing the six earthquake events in the actual six pseudo dynamic tests. The cumulative deformations computed from the analytical and experimental results show that the BRBs at the 3<sup>rd</sup> floors are much more vulnerable than those in the 1<sup>st</sup> and 2<sup>nd</sup> floor. These analytical results also suggest that the inelastic rotational demands imposed on the beam-to-column moment connections of all exterior columns are greatly reduced. All of moment connections survived all the tests without failure.

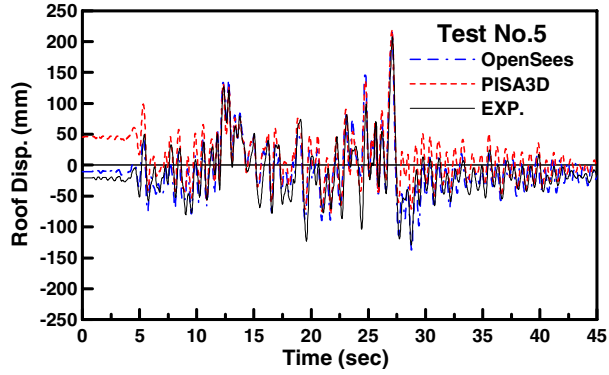


Fig. 19 Roof displacement time history in Test No.5

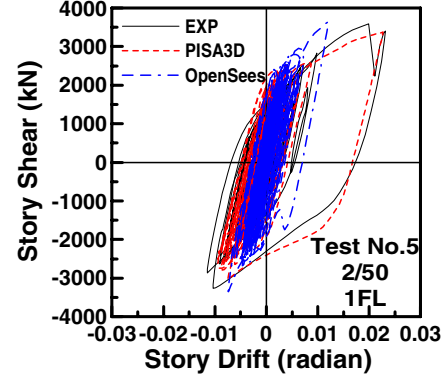


Fig. 20 Hysteresis of 1<sup>st</sup> Story in Test No.5

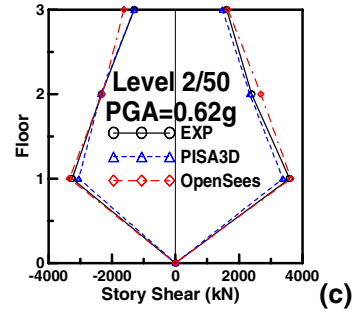
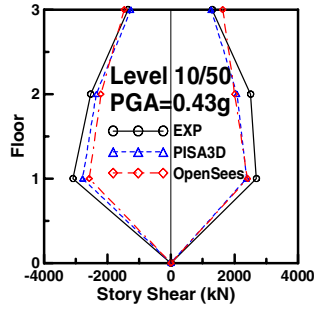
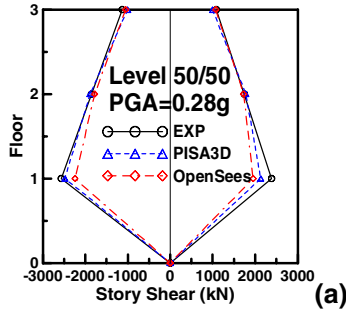


Fig.21 Peak story shear distribution of CFT/BRB frame specimen (a)50/50(b)10/50(c)2/50

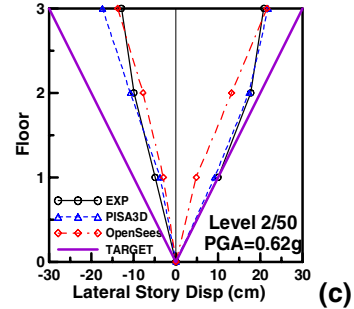
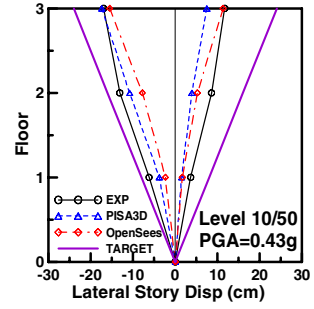
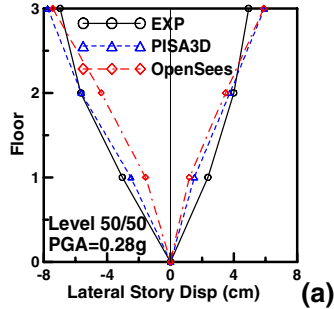


Fig.22 Peak story displacement distribution of CFT/BRB frame specimen (a)50/50(b)10/50(c)2/50

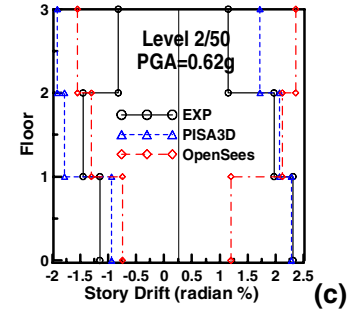
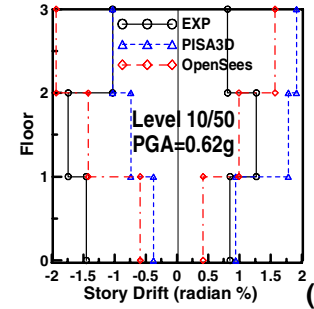
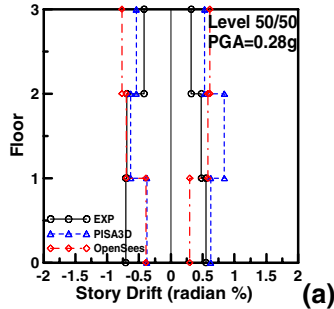


Fig.23 Peak inter-story drift distribution of CFT/BRB frame specimen (a)50/50(b)10/50(c)2/50

Table 6 CPD of BRB members predicted by PISA3D before pseudo tests

	50/50		10/50-I		2/50		10/50-II		Sum	
	N	S	N	S	N	S	N	S	N	S
3 <sup>rd</sup> Floor	1.88	2.18	17.6	18.3	33.2	28.7	16.1	14.8	68.8	64.0
2 <sup>nd</sup> Floor	3.52	3.39	13.5	14.4	26.8	25.2	12.5	12.7	56.3	55.7
1 <sup>st</sup> Floor	0.63	0.55	2.72	2.57	14.1	14.0	3.57	4.29	21.0	21.4

**Table 7 CPD of BRB members evaluated after pseudo tests**

	Test No.1		Test No.2		Test No.3		Test No.4		Test No.5		Test No.6		Sum	
	N	S	N	S	N	S	N	S	N	S	N	S	N	S
3 <sup>rd</sup> Floor	0.80	0.55	1.88	2.18	17.6	18.3	8.45	10.6	33.2	28.7	16.1	14.8	78.0	75.3
2 <sup>nd</sup> Floor	0.13	0.11	3.52	3.39	13.5	14.4	3.81	6.38	26.8	25.2	12.5	12.7	60.3	62.2
1 <sup>st</sup> Floor	0.00	0.01	0.63	0.55	2.72	2.57	1.06	1.55	14.1	14.0	3.57	4.29	22.1	23.0

## CONCLUSIONS

Based on these analyses, summary and conclusions are made as follows:

- The peak story drift is likely to reach 0.025 radian after applying the 2/50 design earthquake on the specimen.
- Tests confirmed that the PISA3D and OpenSees analyses predicted the experimental peak shears extremely well. Experimental peak lateral floor displacements well agree with the prescribed target design responses for both the 10/50 and 2/50 two events.
- Tests also confirmed that experimental peak inter-story drifts of 0.019 and 0.023 radians well agree with the target design limits of 0.02 and 0.025 radians prescribed for the 10/50 and 2/50 events, respectively.
- These analytical results also suggest that the inelastic rotational demands imposed on the beam-to-column moment connections of all exterior columns are greatly reduced. All of moment connections survived all the tests without failure.

## ACKNOWLEDGEMENTS

The National Science Council of Taiwan provided the financial support for this experimental research program. Nippon Steel Company donated two unbonded braces which have been installed in the 2<sup>nd</sup> floor of the frame specimen. The laboratory supports provided by the NCREC are very much appreciated. Valuable suggestions provided by many Taiwan and US professors on this joint effort are gratefully acknowledged.

## REFERENCES

1. Chen, C.H., Lai, W.C. Cordova, P., Deierlein, G. G. and Tsai, K.C., "Pseudo-Dynamic Test of a Full-Scale RCS Frame: Part 1 – Design, Construction and Testing." *Proceedings*, International workshop on Steel and Concrete Composite Constructions, Taipei, Oct. 2003.
2. Yang, Y.S., Wang, S.J., Wang, K.J., Tsai, K.C. and Hsieh, S.H., "ISEE: Internet-Based Simulations for Earthquake Engineering Part I: The Database Approach." *Proceedings*, International workshop on Steel and Concrete Composite Constructions, Taipei, Oct. 2003.
3. Tsai, K.C., and Lin, B.Z., "User Manual for the Platform and Visualization of Inelastic Structural Analysis of 2D Systems PISA3D and VISA3D." Center for Earthquake Engineering Research, National Taiwan University, *Report No. CEER/R92-04*, 2003.
4. ABRI, "Draft Provisions and Commentary for Seismic Regulations for Buildings" 2002.(in Chinese)
5. AISC(American Institute of Steel Construction), "Seismic Provisions for Structural Steel Buildings." Chicago, IL, 1997.
6. CEN, "Design of Composite Steel and Concrete Structures-Part 1-1: General Rules and Rules for Buildings." EuroCommittee for Standardization, Brussels, Belgium, 1992.

7. Loeding, S., Kowalsky, M.J., and Priestley, M.J.N., "Displacement-based Design Methodology Applied to R.C. Building Frames." *Structural Systems Research Report SSRP 98/08*, Structures Division, University of California, San Diego, 1998.
8. Medhekar, M. S. and Kennedy, D. J. L., "Displacement-Based Seismic Design of Buildings-Theory." *Engineering Structures*, 2000; 22(3): 201-209.
9. Newmark, N. M. and Hall, W. J., "Earthquake Spectra and Design." Earthquake Engineering Research Institute, Berkeley, Calif., 1982.
10. Weng, Y.T. (2003) "A Study of Multi-mode Seismic Performance-based Evaluation and Displacement-based Design Procedures." *Ph.D. Thesis*, Supervised by Prof. Keh-Chyuan Tsai, Department of Civil Engineering, National Taiwan University, Taipei, Taiwan, 2003.
11. Tsai, K.C. and Lin, S.L., "A Study of All Metal and Detachable Buckling Restrained Braces." Center for Earthquake Engineering Research, National Taiwan University, *Report No. CEER/R92-03*, 2003.
12. CSI Inc., "SAP2000N, Integrated Finite Element Analysis and Design of Structures." Computer and Structures, Inc., Berkeley, California, USA, 1997.
13. Tsai, K.C., Hwang, Y.C., Weng, C.S., Shirai, T., and Nakamura, H., "Experimental Tests of Large Scale Buckling Restrained Braces and Frames." *Proceedings, Passive Control Symposium 2002*, Tokyo Institute of Technology, Tokyo, December 2002.
14. Tsai, K.C., Lin, M.L., Lin, Y.S. and Wei, S.S., "Nonlinear Responses of Double-Skin Concrete Filled Steel Tube Bridge Pier-to-Foundation Joints." *Journal of Earthquake Engineering and Engineering Seismology*."(in preparation)
15. Chen, C.H., Hsiao, P.C., Lai, J.W., Lin, M.L., Weng, Y.T. and Tsai, K.C., "Pseudo-Dynamic Test of a Full-Scale CFT/BRB Frame: Part 2 - Construction and Testing." Vancouver, Canada. Paper No. 2175, 2004.
16. Lin, M.L., Weng, Y.T., Tsai, K.C., Hsiao, P.C., Chen, C.H. and Lai, J.W., "Pseudo-Dynamic Test of a Full-Scale CFT/BRB Frame: Part 3 - Analysis and Performance Evaluation." Vancouver, Canada. Paper No. 2173, 2004.
17. Sabelli, R., Mahin, S. and Chang, C., "Seismic Demands on Steel Braced Frame Buildings with Buckling-Restrained Braces." *Engineering Structures*, 2000; 25(2): 655-666.